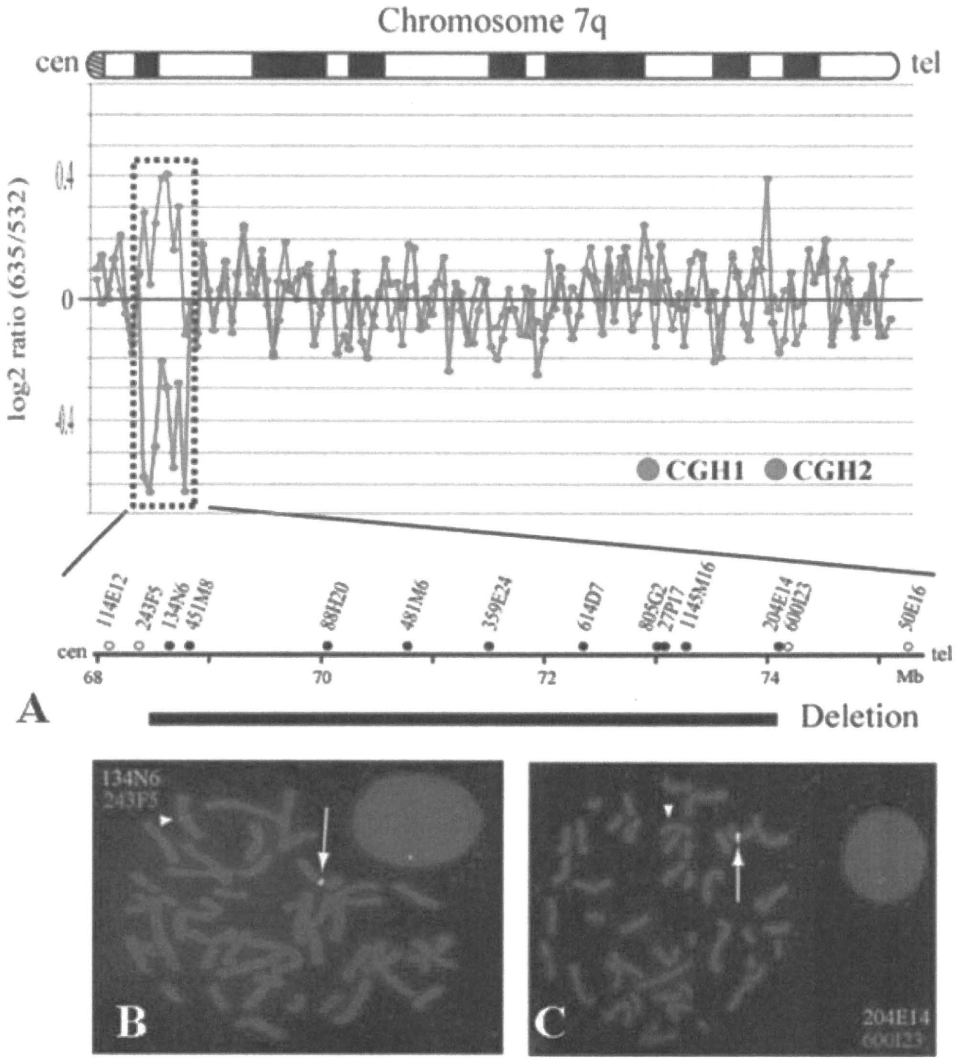

FIG. 1. Molecular cytogenetic analysis of the deletion of 7q11.23 in patient 1 using BAC aCGH and FISH analyses. **A:** aCGH analysis of chromosome 7q. Results are presented below the ideogram of 7q. Patient DNA labeled with Cy5 and normal control DNA labeled with Cy3 was used to obtain the CGH1 data (red), and the CGH2 data (green) was obtained using the same DNAs with the dye labels reversed. The dashed box indicates deleted clones, and is expanded below to give detailed information of the BAC clones used in this study (UCSC Genome Browser coordinates, build 36). Filled circles represent deleted BACs, and open circles represent clones that were not deleted. (**B**, **C**) Chromosomal FISH analyses. Arrows depict visible signals and arrowheads depict absence of signal.

Identification of Zebrafish *hip1*

Although several genes exist in the expanded deletion region of chromosome 7q11.23 in patient 2, there are two candidate genes normally expressed in the brain and therefore potentially responsible for the observed symptoms; i.e. tyrosine 3-monooxygenase/tryptophan 5-monooxygenase activation protein, gamma (14-3-3gamma; YWHAG) gene and the huntingtin-interacting protein 1 (HIP1) gene.

To study whether the deletion of these loci have any relation to infantile spasms and cardiomegaly, we used zebrafish as a model organism. In zebrafish, a homolog of mammalian *HIP1* has yet to be experimentally isolated, but its sequence has been predicted from genomic information. Therefore, for functional analysis, we cloned and identified the cDNA encoding zebrafish *hip1*. Using a reverse transcription (RT)-polymerase chain reaction (PCR)-based strategy, we obtained a full-length open reading frame (ORF) of zebrafish *hip1*, consisting of 3,141 bases and encoding 1,047 amino acids (Accession #AB494966). Zebrafish Hip1 protein has 70% identity to its human and mouse homologs. In addition, in silico software pfam analysis (http://pfam.sanger.ac.uk) revealed that zebrafish *Hip1* contains an N-terminal ANTH/ENTH domain and a C-terminal I/LWEQ domain, both of which are conserved in human *HIP1* (Bhattacharyya *et al.,* 2008). Collectively, these results suggest that *hip1* identified in this study is the zebrafish homolog of mammalian *HIP1* structurally and functionally.

Table 1
Summary of FISH Analyses

BAC clone	Coverage	Location			Patient 1	Patient 2
		Band	Start	End		
RP11-114E12		7q11.22	68,036,962	68,208,211	no deletion	
RP11-243F5		7q11.22	68,389,193	68,579,447	no deletion	
RP11-134N6	*AUTS2*	7q11.22	68,597,691	68,766,491	del	
RP11-88H20		7q11.22	70,101,386	70,101,595	del	
RP11-481M6	*CALN2*	7q11.22	70,766,345	70,944,325	del	
RP11-193J17		7q11.22	71,257,317	71,371,995		marker
RP11-359E24		7q11.22	71,495,966	71,682,413	del	
RP11-479C13		7q11.23	71,883,286	72,073.394		no deletion
RP11-396K3		7q11.23	71,903,765	72,538,417		no deletion
RP11-483G21		7q11.23	72,326,667	72,513,882		del
RP11-614D7		7q11.23	72,375,570	72,564,868	del	
RP11-622P13	*STAX1A*	7q11.23	72,639,987	72,819,209		del
RP11-805G2		7q11.23	73,047,721	73,249,220	del	
	ELN	7q11.23	73,080,363	73,122,172		
RP11-27P17	*LIMK1*	7q11.23	73,122,968	73,290,039	del	
RP11-7M12		7q11.23	73,249,265	73,431,303		del
RP11-1145M16		7q11.23	73,330,134	73,491,216	del	
RP11-247L6		7q11.23	73,510,529	73,676,067		del
RP11-137E8		7q11.23	73,528,656	73,767,523		del
RP11-201E14		7q11.23	74,108,105	74,267,152	del	
RP11-600I23		7q11.23	74,240,609	74,341,149	del	
RP11-99J9	*HIP1*	7q11.23	74,964,894	75,145,939		del
RP11-845K6		7q11.23	75,055,521	75,239,517		del
RP11-50E16		7q11.23	75,362,579	75,520,752	no deletion	
RP11-229D13		7q11.23	75,401,774	75,583,095		del
RP11-951G4	*YWHAG*	7q11.23	75,607,193	75,807,597		del
RP11-340A14		7q11.23	75,968,235	76,028,838		del
RP11-87O14		7q11.23	76,306,441	76,490,214		del
RP11-467H10		7q11.23	76,490,656	75,587,315		no deletion

Genome location corresponds to the March 2006 human reference sequence (NCBI Build 36).
del: deletion

For functional analysis of zebrafish *hip1*, we chose a gene knockdown strategy using morpholino antisense oligos (MOs). Because this approach requires precise nucleotide sequence information of the 5′-untranslated region (UTR), we performed 5′ rapid amplification of cDNA ends (RACE) to determine the sequence of the 5′-UTR of *hip1* in our zebrafish strain. Several nucleotide fragments, ranging from 121 to 264 bases, corresponding to the region upstream of the translation initiation ATG codon were obtained. The 121-base overlapping sequence of these clones was completely identical, and was of sufficient length to design two nonoverlapping, translation-inhibiting MOs (*hip1*-MO1 and *hip1*-MO2). A 5′-terminal guanine residue on the longest clone, rather than the observed thymine in the genomic sequence, suggested that this 264-bp clone contained the full-length 5′-UTR (Supporting Information Fig. S3). In addition, 386 bases of the 3′-UTR, including the polyadenylation signal and polyA tail, were also cloned. Overall, we identified the complete cDNA sequence of zebrafish *hip1*.

Sequence Analysis of 5′-UTR and Exon-Intron Junctions of Zebrafish *ywhag1*

Although a zebrafish homolog of human *YWHAG* was previously isolated and reported as *ywhag1* (Besser *et al.*, 2007; Pujic *et al.*, 2006; Woods *et al.*, 2005), the 5′-UTR in our zebrafish strain had to be determined to design MOs against zebrafish *ywhag1*. 5′ RACE revealed variation of sequence and length, ranging from 29 to 160 bases, in the 5′-UTR of *ywhag1*. Because the 5′ terminus of the shortest clone contained a guanine residue rather than the adenine residue identified in the other clones, this clone was identified as a full-length clone of the shortest form of the 5′-UTR (Supporting Information Fig. S4). To maximize the effect of the MOs, this shortest sequence was used as a template to design MOs that bind all transcripts of *ywhag1*.

Because the 5′-UTR we cloned was too short and not suited for MO binding, we obtained only one MO for translational inhibition of this gene (*ywhag1*-MO1). Because we needed another MO for splicing inhibition, genomic sequences at exon–intron boundaries were required. However, the whole sequence of *ywhag1* was splitted into two clones, Zv7_NA122 and Zv7_NA727, representing the 5′-terminal region (consisting of the 5′-UTR and the 5′ portion of the ORF [initiator ATG to 87G]) and the 3′-terminal region (the 3′ portion of the ORF [88G to the stop codon] and the 3′-UTR), respectively. According to the information in these sequences, zebrafish *ywhag1* was revealed to be composed of two exons and one intron (Supporting Information Fig. S5). Consequently, we cloned fragments containing the puta-

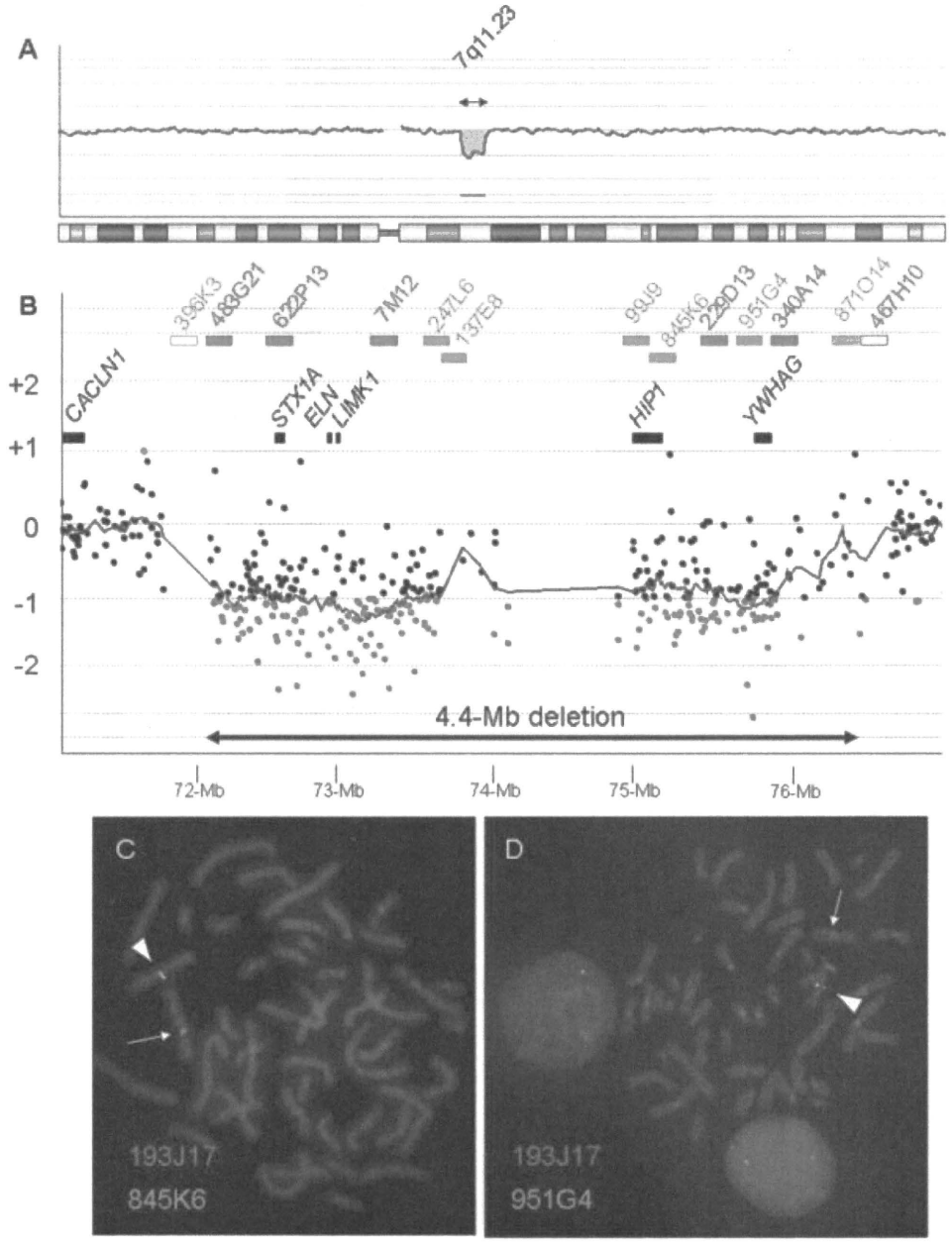

FIG. 2. Molecular cytogenetic analysis of the deletion of 7q11.23 in patient 2 using oligo array CGH and FISH analyses. **A:** Chromosome view indicating loss of genomic copy number in 7q11.23. **B:** Gene View indicating the range of the 4.1-Mb deletion (double-headed arrow, bottom). Black rectangles indicate the locations of known genes within the deletion region. Red and green rectangles indicate the locations of the BAC clones used for FISH analyses. Closed and open rectangles indicate deletion and no deletion, respectively. (C, D) FISH analyses indicating deletion of the green signals (arrows) of RP11-845K6 (C) and RP11-951G4 (D).

tive junction of exon 1/intron 1 and intron 1/exon 2 (Supporting Information Fig. S5), and designed *ywhag1*-spMO.

Zebrafish hip1 Plays No Obvious Role in Brain Development

To confirm whether the deletion of *HIP1* contributes to the phenotype of patient 2, we performed gene knockdown analysis of *hip1* in zebrafish. Microinjection of a small amount (3 ng) of *hip1*-MO1 reduced the yolk extension without any other remarkable phenotypes (Fig. 3E,F) compared with wild type and control MO-injected zebrafish (Fig. 3A–D). By a high dose (5 ng) injection of *hip1*-MO1, the morphants showed complete absence of yolk extension, a narrow body along the dorsoventral axis, and mandibular hypoplasia (Fig. 3G,H). To verify whether these phenotypes were specific for

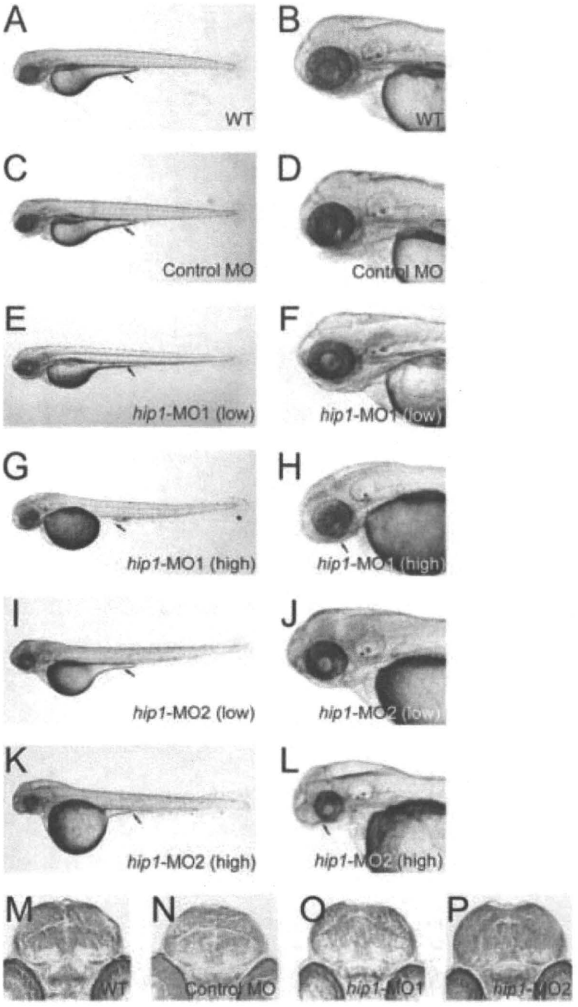

FIG. 3. Zebrafish *hip1* has no evident role in brain development. Morphological observation of wild type (WT) (**A**, **B**), control (**C**, **D**), *hip1*-MO1 morphant (E, F, G, H), and *hip1*-MO2 morphant (**I**, **J**, **K**, **L**) embryos at 72 hpf. Gene knockdown of *hip1* using a low dose (3 ng) of MOs caused reduction of yolk extension (arrow in A, C, **E**, I), whereas a high dose (5 ng) resulted in complete lack of yolk extension, narrow body width, and mandibular agenesis (**G**, **H**, K, L). Arrows indicate yolk extension (G, K) and diminished lower jaw (H, L). Cross-sections of the midbrain in wild type (**M**), control (**N**), *hip1*-MO1 morphant (**O**) and *hip1*-MO2 morphant (**P**) embryos at 72 hpf. All images are displayed with dorsal to the top; A-L are displayed with rostral to the left.

knockdown of *hip1*, the other translation-inhibiting MO, *hip1*-MO2, was used. Similar to *hip1*-MO1 morphants, *hip1*-MO2 morphants showed dose-dependent phenotypes, including reduced yolk extension with no other defects when 3 ng of *hip1*-MO2 was injected (Fig. 3I,J), and complete absence of yolk extension, narrow body along the dorsoventral axis, and severe mandibular aplasia when 5 ng of *hip1*-MO2 was injected (Fig. 3K, L). In addition to these common phenotypes, *hip1*-MO2 morphants also displayed dysplasia of the brain with low penetrance at the higher dose (Fig. 3L), suggesting that this cerebral defect was not the result of specific action of *hip1* knockdown. To examine this, we prepared serial cross-sections of the head of both morphants treated with the low MO dose. If *hip1* had any primary function in brain development, some sort of alteration would likely have occurred in the brain of morphants following injection of a low dose of *hip1* MOs. Although whole brains (from the prosencephalon to the rhombencephalon and along the anteroposterior axis) of embryos at 72 hours post-fertilization (hpf) were cut into serial sections and compared each other, no differences between morphants and wild type or control embryos were observed in any area of the brain (e.g., Fig. 3M–P; corresponding to middle of midbrain). These results indicate that gene knockdown of *hip1* has no obvious effect on the developing brain, although the possibility of involvement of *hip1* was not completely omitted.

Zebrafish ywhag1 Contributes to Brain and Heart Development

It has been reported that, during embryonic development of zebrafish, *ywhag1* is expressed in the head, especially in the diencephalon, tegmentum, and hindbrain (Besser *et al.*, 2007). This expression pattern suggests possible functions of this gene in cerebral and neural growth. Therefore, to investigate whether *ywhag1* has a role in brain development or any relationship to the symptoms of patient 2, we performed gene knockdown of *ywhag1*. Compared with wild type and control embryos (Fig. 4A–D), the *ywhag1*-MO1 morphants (Fig. 4E,F) showed hypomorphic heads and enlarged heart tubes, whereas trunk development was not affected. To confirm that these defects were caused by *ywhag1* knockdown, the splice-inhibiting *ywhag1*-spMO was used. Microinjection of *ywhag1*-spMO drastically reduced mRNA level of *ywhag1* (Supporting Information Fig. S6), and resulted in morphants with a severely hypomorphic head phenotype and enlargement of the heart tube (Fig. 4G,H) similar to *ywhag1*-MO1 morphants (Fig. 4E,F). To gain more confidence, we tested whether coinjection of two MOs at low levels elicits synergistic effect. The quarter amount of each MO (0.75 ng of *ywhag1*-MO1 and 1 ng of *ywhag1*-spMO) that did not cause any obvious defects (data not shown) was coinjected into embryos. Morphant coinjected with these two MOs (*ywhag1*-spMO1+spMO) showed similar phenotypes common to *ywhag1*-MO1- and *ywhag1*-spMO-morphants (Fig. 4I,J). This result indicated that these two MOs exerted the synergistic effect in coinjected embryos (*ywhag1*-spMO1+spMO), and that *ywhag1* is required for normal development of the brain and the heart.

For further investigation of the brain and the heart aberrations in the morphant embryos, serial sections of the head and the heart were examined. Based on the expression pattern of *ywhag1*, we focused on the brain sections containing the diencephalon and midbrain tegmentum (Besser *et al.*, 2007). Compared with wild type and control embryos (Fig. 4K–N), *ywhag1* morphants

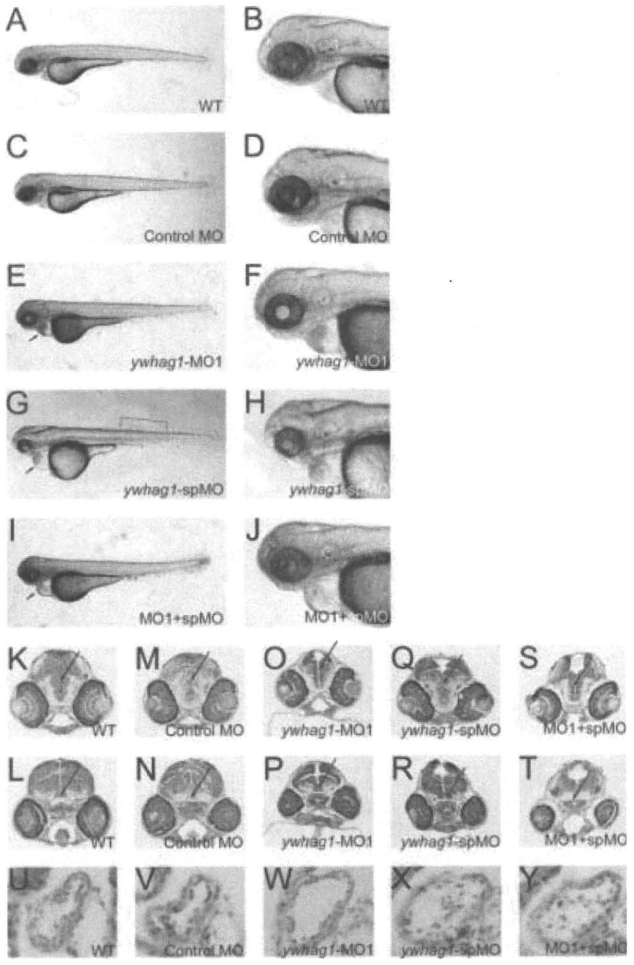

FIG. 4. Zebrafish *ywhag1* is required for development of the brain and the heart. Morphological observation of wild type (WT) (**A**, **B**), control MO morphant (**C**, **D**), *ywhag1*-MO1 morphant (E, F), *ywhag1*-spMO morphant (**G**, **H**) and *ywhag1*-MO1+*ywhag1*-spMO morphant (**I**, **J**) embryos at 72 hpf. Gene knockdown of *ywhag1* caused developmental abnormalities of the head and the enlarged heart tube. Three types of *ywhag1* morphants showed hypomorphic head (**E–J**). Although weak malformation of the trunk and the tail were observed only in *ywhag1*-spMO morphants (bracket) (G), this anomaly was likely to be nonspecific. As same as this manner, the reason of enlargements of the heart pericardiums observed in *ywhag1* morphants (arrows) (E, G, I) is obscure. Cross-sections containing the diencephalon (**K**, **M**, **O**, **Q**, **S**) and the midbrain tegmentum (**L**, **N**, O, **R**, **T**) of WT (K, L), control (M, N), *ywhag1*-MO1 morphant (O, **P**) and *ywhag1*-spMO morphant (Q, R) and *ywhag1*-MO1+spMO morphant (S, T) embryos at 72 hpf are shown (arrows). Compared with WT (K, L) and control (M, N), *ywhag1* morphants showed hypomorphic heads. Cross-sections of the heart ventricles in WT (**U**), control (**V**), *ywhag1*-MO1 morphant (**W**), *ywhag1*-spMO morphant (**X**) and *ywhag1*-MO1+spMO morphant (**Y**) embryos at 72 hpf. Compared with WT (U) and control (V), *ywhag1* morphants (W, X, Y) showed enlarged ventricles of the hearts. All images are displayed with dorsal to the top; A-J are displayed with rostral to the left.

exhibited obvious dysplasia of the brain (Fig. 4O–T). In normal cerebral development in the zebrafish, the brain ventricle is narrowed along with the progression of development and almost buried until 72 hpf (Fig. 4K–N). In the knockdown experiments, wild type and control embryos had a solid diencephalon structure (Fig. 4K,M), whereas the diencephalons of all *ywhag1* morphants were divided by the brain ventricle (Fig. 4O,Q,S). Similar abnormal partitions were observed in the tectum opticum (the dorsal upper structure of midbrain tegmentum indicated by arrow; Fig. 4P,R,T). Furthermore, the midbrain tegmentum was not formed properly in morphants (Fig. 4P,R,T). About the heart tube, major diameter of the ventricle was obviously enlarged in *ywhag1* morphants (Fig. 4W,X,Y) compared with wild type and control morphants (Fig. 4U,V). These results strongly indicate that *ywhag1* is important for normal brain and heart development.

Regarding the functions of the heart in all zebrafishes, we measured the pulse rate, and there were no statistically significant differences among all groups of larvae. However, incidence of arrhythmia was significantly elevated in all three types of *ywhag1* morphants (Supporting Information Table S1 and Fig. S7).

Mutation analysis of *HIP1* and *YWHAG* in Patients With Neurological Symptoms

Although total of 142 samples derived from patients with neurological symptoms including developmental delay and/or epilepsy were analyzed for mutation analysis of *HIP1* and *YWHAG*, there was no pathogenic mutation.

DISCUSSION

Because WBS is not usually associated with infantile spasms, genotype-phonotype comparisons in WBS patients with atypically large deletions may assist identification of gene(s) responsible for infantile spasms. Marshall *et al.* (2008) investigated 16 patients associated with documented seizures and interstitial deletions of 7q11.23-q21.1, which is neighboring to the WBS critical region, and revealed overlapping deletions of the *MAGI2* in most patients. However, they reported at least one patient having infantile spasms and a chromosomal deletion including WBS critical region but in which *MAGI2* was not included, who had been reported previously by Morimoto et al. (2003).

In this study, we identified two additional WBS patients with atypically large deletions. Patient 1 had a deletion at 7q11.23 that extended into the proximal region and included three genes; i.e. *AUTS2*, *WBSCR17*, and *CALN1* (Fig. 5, Table 1). Expression of human *CALN1* (*calneuron 1)* is brain specific (Wu *et al.,* 2001), and expression of the mouse homolog in the cerebellum increases from the postnatal 2nd week to day 21, and reaches to adult level. In situ hybridization showed a high level of expression of *CALN1* in the cerebellum, hippocampus, striatum, and cortex (Wu *et al.,* 2001). The postnatal expression pattern in mice is consistent with the onset of infantile spasms in humans, which occurs from 3 to 6 months after birth. *CALN1* shows sig-

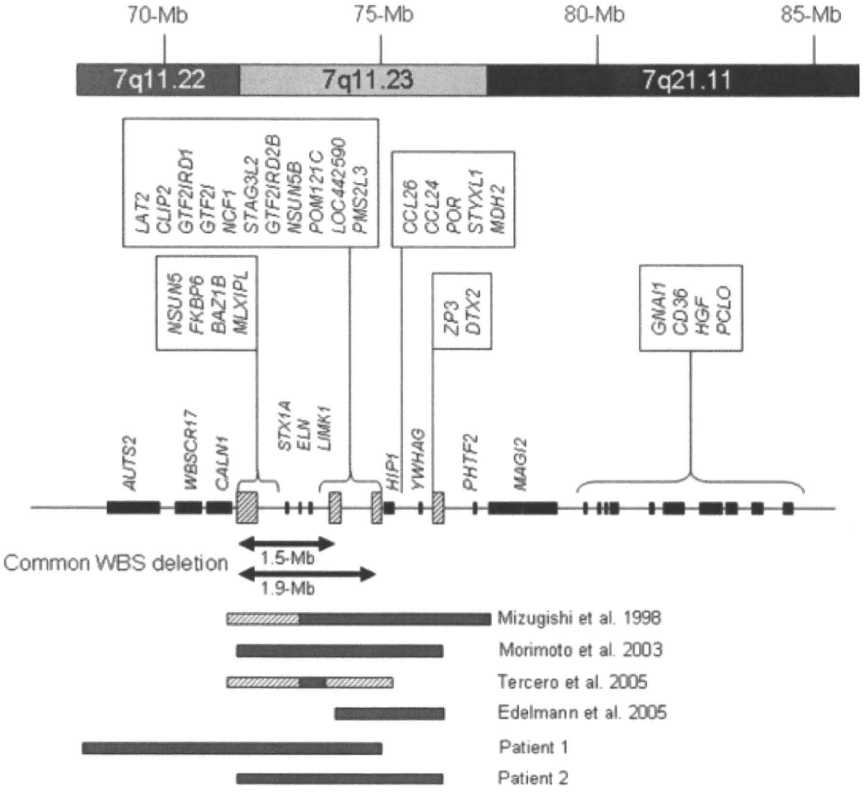

FIG. 5. Chromosome map around the common WBS deletion. Black and hatched rectangles on a horizontal bar indicate the sizes and the locations of genes and duplicated segments, respectively. Gray bars indicate the region of the chromosome deleted in the indicated patient, with the ambiguity indicated as hatched bars.

nificant similarity to members of the calmodulin superfamily (Wu *et al.,* 2001). Thus, haploinsufficiency of *CALN1* may cause the infantile spasms in this patient. *AUTS2* is also a compelling candidate gene for the infantile spasms in patient 1, because it is robustly expressed in the fetal brain and is reported to be interrupted by a translocation breakpoint in patients with autistic behavior or mental retardation (Kalscheuer *et al.,* 2007; Sultana *et al.*, 2002).

Patient 2 had a deletion that extended into the distal telomeric region. The range of this deletion is exactly same as that of the patient reported by Morimoto *et al.* who also showed infantile spasms and cardiomegaly (Morimoto *et al.*, 2003) (see Fig. 5). At the telomeric breakpoint, there is a region of duplicated segments. This telomeric breakpoint was also shared by a patient reported by Edelmann *et al.* (2007), who presented with autism associated with a chromosomal deletion of 7q11.23, which did not include *ELN* but expanded into the telomeric region beyond the WBS critical region (see Fig. 5). These common breakpoints indicate that this region of duplicated segments can act as a LCR for nonhomologous allele recombination (NHAR).

There are 9 genes in the expanded deletion toward the telomeric region neigboring the WBS critical region (see Fig. 5). Among them, Edelmann *et al.* (2007) focused on *HIP1* and *YWHAG* as the prime candidates responsible for autism seen in their patient, and analyzed the expression levels of them by RT-PCR method. Then, they revealed reduced expression of *YWHAG* in transformed lymphocytes derived from the patient, but no decrease in *HIP1*. Based on these findings, we analyzed the function of *HIP1* and *YWHAG* using a gene knockdown system in zebrafish, and the correlation with neurological functions.

In this study, the zebrafish *hip1* knockdown did not show significant abnormality, which is consistent with previous reports of *Hip1*-deficient mice. Homozygous *Hip1-/-* mice generated by targeted deletion exhibited degeneration of the seminiferous tubules of the testis with excessive apoptosis of postmeiotic spermatids, but these mice developed to adulthood and did not show overt neurologic symptoms (Rao *et al.*, 2001). In addition, mice with different deletions of *hip1* showed hematopoietic abnormalities, spinal defects, and cataracts due to cell death in the lens, but had no notable cerebral or neurological anomalies (Oravecz-Wilson et al., 2004).

In contrast, reduced brain size and enlargement of the heart tube were observed when *ywhag1* was knocked down in zebrafish. This indicates that the infantile spasms and the cardiomegaly observed in patient 2 might be derived from haploinsufficiency of *YWHAG*,

because the WBS patient reported by Morimoto *et al* (2003). also showed infantile spasms and cardiomegaly. *YWHAG* binds to *protein kinase C alpha (PRKCA) and p53* is directly phosphorylated by *PRKCA*, which is crucial for activation of *p53 protein* (Autieri and Carbone, 1999; Price and Youmell, 1997). 14-3-3 proteins including *YWHAG* modulate cell survival and control apoptosis (Morrison, 2009; Porter *et al.*, 2006) and inhibition of physical binding between 14-3-3 and its ligand proteins causes apoptosis (Masters and Fu, 2001). Therefore, the etiology of hypoplastic brain in the zebrafish model might be the consequence of apoptic cell death in central nervous system at early development. Regarding the involvement of the heart, we observed arrhythmia in *Ywhag1* knockdown zebrafish and the incidence of arrhythmia in *ywhag1* knockdown zebrafish is worth noting. Although patient 2 did not show arrhythmia, it might be masked by medication with beta-blockers. Since we did not identify any mutations in patients with mental retardation and/or epilepsy, no definitive evidence of a link between *HIP1/YWHAG* haploinsufficiencies and neurological symptoms was obtained. However, given the evidence reported herein, *YWHAG* are promising candidate genes for infantile spasms.

In conclusion, we have described two new WBS patients that presented with infantile spasms and had atypically large deletions in 7q11, one extending into the proximal side of the common WBS deletion and one extending into the telomeric side. In the telomeric side, we identified two promising candidate genes, *HIP1* and *YWHAG*. Using a knockdown approach, we showed that a loss of zebrafish *ywhag1* leads to brain development delay and heart tube enlargement. Because the patient with haploinsufficiency of *YWHAG* showed infantile spasms and cardiomegaly, *YWHAG* may have important roles in both brain and heart development. Although there was no *YWHAG* mutation identified in the patients with mental retardation and/or epilepsy, this gene is a noteworthy candidate for epilepsy, along with *AUTS2*, *CALN1*, and *HIP1*.

MATERIALS AND METHODS

Subjects

After obtaining informed consents based on a permission approved by the institution's ethical committee, peripheral blood samples were obtained from the patients and their parents.

For genomic mutation screening for *HIP1* and *YWHAG*, we used 142 DNA samples derived from 128 and 14 patients with idiopathic mental retardation with and without epilepsy, respectively. Etiologies of all these patients were unknown and were negated to have genomic copy number aberrations using aCGH (Shimojima *et al.*, 2009b). In 128 patients with epilepsy, there were 5 patients with early infantile epileptic encephalopathy, 43 patients with West syndrome, and 2 patients with Lennox-Gastaut syndrome. All of the 14 nonepileptic patients showed cerebral dsygenesis including gyrus malformation, brain atrophy, and microcephaly.

aCGH Analysis

For aCGH analysis of patient 1, we used the originally developed microarray in which 5,057 BAC/PAC clones were plotted. We selected probes using the UCSC Genome Browser (http://genome.ucsc.edu) spaced every 0.7 Mb across the whole human genome, and chose 4,235 clones that showed a unique FISH signal at the predicted chromosomal location. A total of 822 clones were not subjected to aCGH analysis; 438 (8.7%) yielded multiple chromosomal signals using FISH and 384 (7.6%) showed aberrant FISH signals likely due to contamination in our laboratory. Fifty-nine BAC/PAC clones, previously used for subtelomere and syndromic-MR-specific microarray analysis, were among the 4,235 clones (Harada *et al.*, 2004; Kurosawa *et al.*, 2004). BAC/PAC DNA was extracted using the PI-100 automatic DNA extraction system (Kurabo, Osaka, Japan), subjected to two rounds of PCR amplification, purified, adjusted to a final concentration of >500 ng/μl, and spotted in duplicate on CodeLinkTM activated slides (Amersham Biosciences Corp, Piscataway, NJ) using the ink-jet spotting method (Nihon Gaishi, Nagoya, Japan) as described previously (Miyake *et al.*, 2006). aCGH analysis was performed using 4,235 BAC arrays. After complete digestion using *DpnII*, CGH1 was set up using subject DNA labeled with Cy-5-dCTP (Amersham Biosciences) and reference DNA labeled with Cy-3-dCTP (Amersham Biosciences) using a DNA random primer kit (Invitrogen, Carlsbad, CA). To rule out false positives, dyes were swapped in the CGH2 set (subject DNA was labeled with Cy3 and reference DNA was labeled with Cy5), such that the signal patterns of CGH1 were reversed. Prehybridization and hybridization were performed as described previously (Harada *et al.*, 2004). The arrays were scanned by GenePix 4000B (Axon Instruments, Union City, CA) and analyzed using GenePix Pro 6.0 (Axon Instruments). The signal intensity ratio between subject and control DNA was calculated from the data of the single-slide experiment in each for CGH1 and CGH2, using the ratio of means formula (F635 Mean-B635 Median/F532 Mean-B532 Median) according to GenePix Pro. 6.0. The standard deviation of each clone was calculated. The signal intensity ratio was considered significant if it was greater than three standard deviations from the mean in both the CGH1 and CGH2 sample sets.

For patient 2, genomic copy number aberrations were analyzed using the Human Genome CGH Microarray 105A chip (Agilent Technologies, Santa Clara, CA) according to methods described elsewhere (Shimojima *et al.*, 2009a). Briefly, 500 ng genomic DNA was extracted from peripheral blood of the patient and the reference individual, using the QIAquick DNA extraction kit (QIAgen, Valencia, CA), and was digested with restriction enzymes. Cy-5-dUTP (patient) or Cy-3-dUTP (reference) was incorporated using the Klenow frag-

ment. The array was hybridized in the presence of Cot-1 DNA and blocking agents for 40 hours at 65°C, washed, and scanned by GenePix 4000B (Axon Instruments). Data were extracted w Agilent Feature Extraction software version 9 using default settings for CGH. Statistically significant aberrations were determined using the ADM-II algorithm in the CGH analytics version 3.5 (Agilent Technologies). Breakpoints were defined as the start and stop location of the first and last probes, respectively, included in the algorithmically determined region of deletion.

FISH Analysis

Metaphase or prometaphase chromosomes were prepared from phytohemagglutinin-stimulated peripheral blood lymphocytes according to standard techniques. RP11 BAC clones were selected from in silico library build 2006 and were purchased from Invitrogen (Table 1).

FISH analyses using the combination with two BAC clones were performed according to the following method. After hardening chromosome slides at 65°C for 150 min, they were denatured in 70% formamide containing 2× standard saline citrate (SSC) at 70°C for 2 min, and then dehydrated at −20°C in ethanol. BAC clone DNA was extracted using GenePrepStar PI-80X (Kurabo) and labeled with SpectrumGreen TM-11-dUTP or SpectrumOrange TM-11-dUTP (Vysis, Downers Grove, IL) by nick translation and then denatured at 70°C for 5 min. The probe-hybridization mixture was applied to the chromosomes, which were incubated at 37°C for 16 h. Slides were washed twice in 50% formamide containing 2× SSC at 43°C for 15 min, then in 2× SSC for 5 min, 1× SSC for 5 min, 0.1% Triton X-100 containing 4× SSC for 5 min with shaking, 4× SSC for 5 min and 2× SSC for 5 min. Slides were then mounted in antifade solution (Vector Laboratories, Burlingame, CA) containing 4′,6-diamino-2-phenylindole (DAPI). Fluorescence photomicroscopy was performed as described previously (Miyake *et al.*, 2003).

Mutation Screening of *HIP1* and *YWHAG* Coding Regions

All exons of *HIP1* and *YWHAG* (21 and 3 total exons, respectively) were amplified by PCR using originally designed primers derived from the neighboring intronic sequences of each exon (Supporting Information Tables S2 and S3), according to standard methods. All amplicons were subjected to direct sequencing using the BigDye terminator cycle sequencing kit (Applied Biosystems, Carlsbad, CA) according to the manufacturer's protocol. Sequencing results were analyzed using the 3130xl Genetic Analyzer (Applied Biosystems).

Zebrafish Maintenance

Adult zebrafish (Danio rerio) were maintained at 28.5°C under 14-hr light/10-hr dark cycle conditions. Fertilized eggs from natural crosses were collected a few minutes after spawning and cultured at 28.5°C in water containing 0.006% NaCl and 0.00025% methylene blue. Embryos were staged according to morphology and hours post-fertilization (hpf) as described (Kimmel *et al.*, 1995). N-Phenylthiourea was added to culture water at a final concentration of 0.003% to avoid pigmentation of larvae.

Sequence Analyses of Zebrafish *hip1* and *ywhag1*

The nucleotide sequence of *hip1* cDNA has been predicted from the genomic information of zebrafish. The cDNA corresponding to the ORF of *hip1* was experimentally cloned by RT-PCR using primers designed based on the predicted sequence. The 5′- and 3′-UTRs of *hip1* were also cloned by RACE. To design antisense MOs against *ywhag1*, the 5′-UTR in our zebrafish strain, Michigan, was cloned using 5′ RACE. Then, the cDNA sequence, Accession #NM_21302, was obtained from GenBank (http://www.ncbi.nlm.nih.gov/Genbank). In addition, fragments surrounding the exon-intron junctions of *ywhag1*, including the putative exon 1/intron 1 and intron 1/exon 2 junctions, were amplified by PCR using genomic DNA as a template and primers corresponding to the zebrafish whole-genome shotgun scaffolds Zv7_NA122 and Zv7_NA727. Total RNA was extracted from embryos 24-hpf using the RNeasy Mini Kit (QIAgen), and cDNA was synthesized using the Omniscript RT Kit (QIAgen) according to the manufacturer's instructions. Extraction of genomic DNA from adult zebrafish was performed as described (Westerfield, 1995). All PCR amplification reactions were performed using KOD plus DNA polymerase (Toyobo, Osaka, Japan). For 5′ RACE, the 5′-RACE Core Set (Takara, Otsu, Japan) was used. The sequences of the primers used in this study are shown in Supporting information Table S4.

Morpholinos and Microinjection

MOs were purchased from Gene Tools (Philomath, OR). For gene knockdown of *hip1*, two nonoverlapping translation-inhibiting MOs (*hip1*-MO1, *hip1*-MO2) were used. For *ywhag1*, one translation-inhibiting MO (*ywhag1*-MO1) and one splice-inhibiting MO (*ywhag1*-spMO) were employed. As a negative control, a standard control MO was used. The sequences of these MOs are shown in Supplemental Table S4. MOs were resuspended at 10 μg/μl in Danieau solution (5 mM HEPES, pH 7.6, 58 m*M* NaCl, 0.7 m*M* KCl, 0.4 m*M* $MgSO_4$, and 0.6 m*M* $Ca(NO_3)_2$) and stored at −20°C. Microinjections were performed as described (Razzaque *et al.*, 2007).

Preparation of Zebrafish Head Sections

Zebrafish embryos at the 72 hpf were fixed with 4% paraformaldehyde in PBS at 4°C overnight. The fixed embryos were serially dehydrated in ethanol, soaked in xylene, and embedded in Paraplast Plus embedding medium (McCormick Scientific, St. Louis, MO) under microscopic observation. Specimens were cut into serial sec-

tions (7 μm) and stained with Mayer's hematoxylin and eosin solutions.

LITERATURE CITED

Autieri MV, Carbone CJ. 1999. 14-3-3Gamma interacts with and is phosphorylated by multiple protein kinase C isoforms in PDGF-stimulated human vascular smooth muscle cells. DNA Cell Biol 18:555–564.

Besser J, Bagowski CP, Salas-Vidal E, van Hemert MJ, Bussmann J, Spaink HP. 2007. Expression analysis of the family of 14-3-3 proteins in zebrafish development. Gene Expr Patterns 7:511–520.

Bhattacharyya NP, Banerjee M, Majumder P. 2008. Huntington's disease: Roles of huntingtin-interacting protein 1 (HIP-1) and its molecular partner HIPPI in the regulation of apoptosis and transcription. FEBS J 275:4271–4279.

Edelmann L, Prosnitz A, Pardo S, Bhatt J, Cohen N, Lauriat T, Ouchanov L, Gonzalez PJ, Manghi ER, Bondy P, Esquivel M, Monge S, Delgado MF, Splendore A, Francke U, Burton BK, McInnes LA. 2007. An atypical deletion of the Williams-Beuren syndrome interval implicates genes associated with defective visuospatial processing and autism. J Med Genet 44:136–143.

Ewart AK, Morris CA, Atkinson D, Jin W, Sternes K, Spallone P, Stock AD, Leppert M, Keating MT. 1993. Hemizygosity at the elastin locus in a developmental disorder. Williams syndrome. Nat Genet 5:11–16.

Harada N, Visser R, Dawson A, Fukamachi M, Iwakoshi M, Okamoto N, Kishino T, Niikawa N, Matsumoto N. 2004. A 1-Mb critical region in six patients with 9q34.3 terminal deletion syndrome. J Hum Genet 49:440–444.

Kalscheuer VM, FitzPatrick D, Tommerup N, Bugge M, Niebuhr E, Neumann LM, Tzschach A, Shoichet SA, Menzel C, Erdogan F, Arkesteijn G, Ropers HH, Ullmann R. 2007. Mutations in autism susceptibility candidate 2 (AUTS2) in patients with mental retardation. Hum Genet 121:501–509.

Kimmel CB, Ballard WW, Kimmel SR, Ullmann B, Schilling TF. 1995. Stages of embryonic development of the zebrafish. Dev Dyn 203:253–310.

Kurosawa K, Harada N, Sosonkina N, Niikawa N, Matsumoto N, Saitoh S. 2004. Unmasking 15q12 deletion using microarray-based comparative genomic hybridization in a mentally retarded boy with r(Y). Am J Med Genet A 130A:322–324.

Marshall CR, Young EJ, Pani AM, Freckmann ML, Lacassie Y, Howald C, Fitzgerald KK, Peippo M, Morris CA, Shane K, Priolo M, Morimoto M, Kondo I, Manguoglu E, Berker-Karauzum S, Edery P, Hobart HH, Mervis CB, Zuffardi O, Reymond A, Kaplan P, Tassabehji M, Gregg RG, Scherer SW, Osborne LR. 2008. Infantile spasms is associated with deletion of the MAGI2 gene on chromosome 7q11.23-q21.11. Am J Hum Genet 83:106–111.

Masters SC, Fu H. 2001. 14-3-3 proteins mediate an essential anti-apoptotic signal. J Biol Chem 276:45193–45200.

Miyake N, Kurotaki N, Sugawara H, Shimokawa O, Harada N, Kondoh T, Tsukahara M, Ishikiriyama S, Sonoda T, Miyoshi Y, Sakazume S, Fukushima Y, Ohashi H, Nagai T, Kawame H, Kurosawa K, Touyama M, Shiihara T, Okamoto N, Nishimoto J, Yoshiura K, Ohta T, Kishino T, Niikawa N, Matsumoto N. 2003. Preferential paternal origin of microdeletions caused by prezygotic chromosome or chromatid rearrangements in Sotos syndrome. Am J Hum Genet 72:1331–1337.

Miyake N, Shimokawa O, Harada N, Sosonkina N, Okubo A, Kawara H, Okamoto N, Ohashi H, Kurosawa K, Naritomi K, Kaname T, Nagai T, Shotelersuk V, Hou JW, Fukushima Y, Kondoh T, Matsumoto T, Shinoki T, Kato M, Tonoki H, Nomura M, Yoshiura K, Kishino T, Ohta T, Niikawa N, Matsumoto N. 2006. No detectable genomic aberrations by BAC array CGH in Kabuki make-up syndrome patients. Am J Med Genet A 140:291–293.

Mizugishi K, Yamanaka K, Kuwajima K, Kondo I. 1998. Interstitial deletion of chromosome 7q in a patient with Williams syndrome and infantile spasms. J Hum Genet 43:178–181.

Morimoto M, An B, Ogami A, Shin N, Sugino Y, Sawai Y, Usuku T, Tanaka M, Hirai K, Nishimura A, Hasegawa K, Sugimoto T. 2003. Infantile spasms in a patient with williams syndrome and craniosynostosis. Epilepsia 44:1459–1462.

Morris CA. 2006. Genotype-phenotype correlations in Williams-Beuren syndrome. In: Morris CA, Lenhoff HM, Wang PP, editors. Williams-Beuren syndrome. Baltimore: The Johns Hopkins University Press. pp 59–82.

Morrison DK. 2009. The 14-3-3 proteins: Integrators of diverse signaling cues that impact cell fate and cancer development. Trends Cell Biol 19:16–23.

Oravecz-Wilson KI, Kiel MJ, Li L, Rao DS, Saint-Dic D, Kumar PD, Provot MM, Hankenson KD, Reddy VN, Lieberman AP, Morrison SJ, Ross TS. 2004. Huntingtin Interacting Protein 1 mutations lead to abnormal hematopoiesis, spinal defects and cataracts. Hum Mol Genet 13:851–867.

Porter GW, Khuri FR, Fu H. 2006. Dynamic 14-3-3/client protein interactions integrate survival and apoptotic pathways. Semin Cancer Biol 16:193–202.

Price BD, Youmell MB. 1997. Phosphorylation of the p53 protein regulates its transcriptional activity. In: Proc. 45th Annual Meeting of the Radiation Research Society. Oak Brook, IL. p 57.

Pujic Z, Omori Y, Tsujikawa M, Thisse B, Thisse C, Malicki J. 2006. Reverse genetic analysis of neurogenesis in the zebrafish retina. Dev Biol 293:330–347.

Rao DS, Chang JC, Kumar PD, Mizukami I, Smithson GM, Bradley SV, Parlow AF, Ross TS. 2001. Huntingtin interacting protein 1 Is a clathrin coat binding protein required for differentiation of late spermatogenic progenitors. Mol Cell Biol 21:7796–7806.

Razzaque MA, Nishizawa T, Komoike Y, Yagi H, Furutani M, Amo R, Kamisago M, Momma K, Katayama H, Nakagawa M, Fujiwara Y, Matsushima M, Mizuno K, Tokuyama M, Hirota H, Muneuchi J, Higashinakagawa T, Matsuoka R. 2007. Germline gain-of-function mutations in RAF1 cause Noonan syndrome. Nat Genet 39:1013–1017.

Shimojima K, Adachi M, Tanaka M, Tanaka Y, Kurosawa K, Yamamoto T. 2009a Clinical features of microdeletion 9q22.3 (pat). Clin Genet 75:384–393.

Shimojima K, Komoike Y, Tohyama J, Takahashi S, Paez MT, Nakagawa E, Goto Y, Ohno K, Ohtsu M, Oguni H, Osawa M, Higashinakagawa T, Yamamoto T. 2009b. TULIP1 (RALGAPA1) haploinsufficiency with brain development delay. Genomics 94:414–422.

Stromme P, Bjornstad PG, Ramstad K. 2002. Prevalence estimation of Williams syndrome. J Child Neurol 17:269–271.

Sultana R, Yu CE, Yu J, Munson J, Chen D, Hua W, Estes A, Cortes F, de la Barra F, Yu D, Haider ST, Trask BJ, Green ED, Raskind WH, Disteche CM, Wijsman E, Dawson G, Storm DR, Schellenberg GD, Villacres EC. 2002. Identification of a novel gene on chromosome 7q11.2 interrupted by a translocation breakpoint in a pair of autistic twins. Genomics 80:129–134.

Westerfield M. 1995. A guide for the laboratory use of zebrafish (Danio rerio). Oregon: University of Oregon Press.

Woods IG, Wilson C, Friedlander B, Chang P, Reyes DK, Nix R, Kelly PD, Chu F, Postlethwait JH, Talbot WS. 2005. The zebrafish gene map defines ancestral vertebrate chromosomes. Genome Res 15:1307–1314.

Wu YQ, Lin X, Liu CM, Jamrich M, Shaffer LG. 2001. Identification of a human brain-specific gene, calneuron 1, a new member of the calmodulin superfamily. Mol Genet Metab 72:343–350.

Wu YQ, Sutton VR, Nickerson E, Lupski JR, Potocki L, Korenberg JR, Greenberg F, Tassabehji M, Shaffer LG. 1998. Delineation of the common critical region in Williams syndrome and clinical correlation of growth, heart defects, ethnicity, and parental origin. Am J Med Genet 78:82–89.

Supporting Information

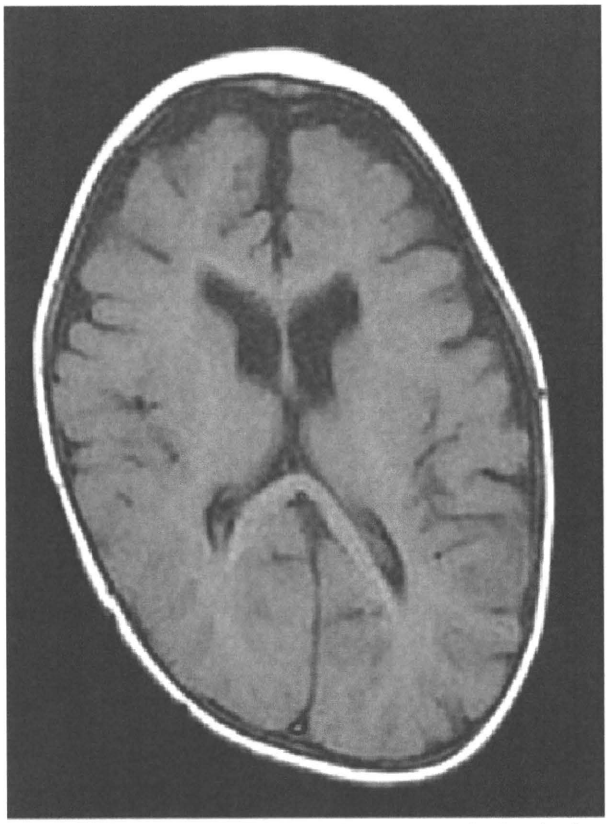

FIG. S1. Brain MRI showing atrophic brain in patient 1 at 8 months of age

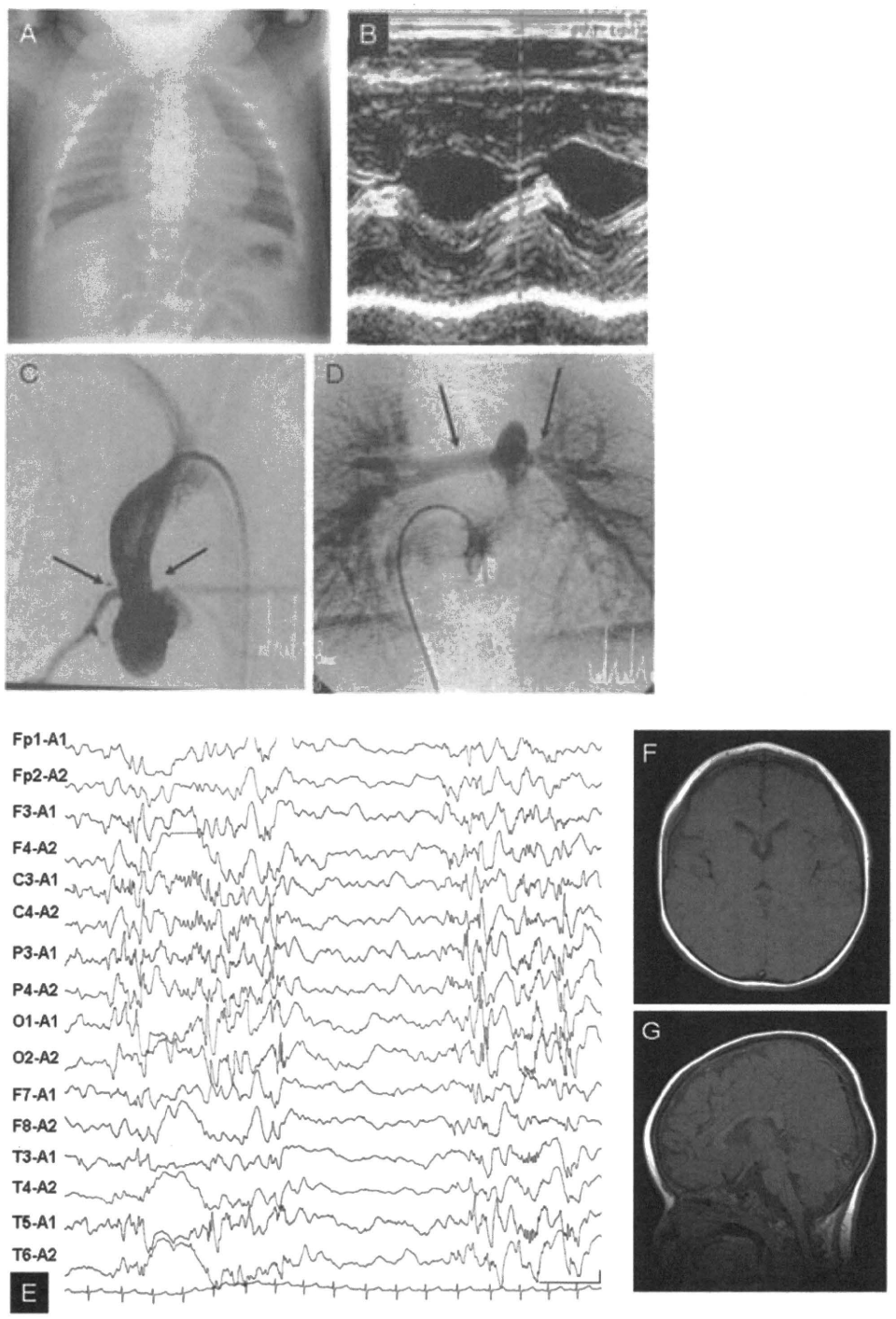

FIG. S2. Clinical examination of patient 2. (A) Chest X-ray indicating cardiac dilatation. (B) Echocardiography displaying prominent hypertrophy of the cardiac muscle in M mode. Due to prominent cardiac hypertrophy, ventricular spaces were not well recognized. Cardiac catheterization examination showed supravalvular aortic stenosis (C, arrows) and peripheral pulmonary stenosis (D, arrows) compatible with that seen in patients with WBS. (E) Electroencephalogram indicating intermittent hypsarrhythmia during sleep stages, causing tonic spasms. Brain MRI showed no abnormal structures or intensities on the axial (F) or sagittal (G) sequences.

```
genome 001:TGTATACCGTCGCTCGCGCGCACTGACGCGCTGTTTTCTCTTGCAGATCT 050
RACE_1 001:G.................................................. 050
RACE_2 001:---------------------------------------------------- 001
RACE_3 001:---------------------------------------------------- 001

genome 051:GTGATTGCGCGCACAGACGCGTGTTTTGCGCGCTCGCGAGCGGAGAGCGG 100
RACE_1 051:.................................................. 100
RACE_2 001:------------...................................... 038
RACE_3 001:---------------------------------------------------- 001

genome 101:AATAGCGCTGGAATGATATCCATGGGCGGTGGACGAGGAAAATGACCTTT 150
RACE_1 101:.................................................. 150
RACE_2 039:.................................................. 088
RACE_3 001:-------------------------------------------..... 007

genome 151:TGTGATAACGACGAGGGCTTGAGATTTTCGTGCTCAACGCTAGAGTCAAC 200
RACE_1 151:.................................................. 200
RACE_2 089:.................................................. 138
RACE_3 008:.................................................. 057

genome 201:ACACTATTTATGTTGATTTAGGAAGTCTTGGTCGCTCGCGCAGCTTGGAC 250
RACE_1 201:.................................................. 250
RACE_2 139:.................................................. 188
RACE_3 058:.................................................. 107

genome 251:TTTTCTTTCCAGAAATGGACCG                            272
RACE_1 251:.....................                            272
RACE_2 189:.....................                            210
RACE_3 108:.....................                            129
```

FIG. S3. Sequence of the 5'-UTR of *hip1*. A red character indicates a cap structure deduced by 5' RACE.

```
RACE_1 001:GCACGTCTTGATCAGGAAGTTGTCGAGGAGGAGGCGCGTCCTGCATCGGC 050
RACE_2 001:-----------------------..................... 026
RACE_3 001:-------------------------------------------... 003
RACE_4 001:------------------------------------------- 001

RACE_1 051:ACGCGTTCAACAGCAGAGAGCAGAGGAAAGAGAAGCGGACAGAGGAGCTT 100
RACE_2 027:.................................................. 076
RACE_3 004:.................................................. 053
RACE_4 001:------------------------------------------------- 001

RACE_1 101:TACAGTCGCCAAAAAAAAAAAAA--CCCTGAGAGCACTCATACTGCACC 148
RACE_2 077:.....................AA..................... 126
RACE_3 054:.....................---..................... 100
RACE_4 001:--------------------------------G.............. 017

RACE_1 149:CCAAAACTGAACATGGTCGA                          168
RACE_2 127:...................                           146
RACE_3 101:...................                           120
RACE_4 018:...................                           037
```

FIG. S4. Sequence of the 5'-UTR of *ywhag1*. A red character indicates a cap structure deduced by 5' RACE.

A

GAGCAGCTGG TGCAGAAAGC CAGACTGGCC GAGCAGGCGG AGAGATATGA
TGATATGGCT GCAGCCATGA AATCGgtaag cgcaactttt gcattatcct
gtatgtcaat tgtataatta ataattacgc aatccgggta gtcattacaa

B

agactttccc aacatcgtga agccctaata ggtgctcttt aaagtaactt
ctttatcttc tctccatctc tttagGTGAC AGAGCTGAAC GAAGCCCTGT
CCAACGAGGA GAGGAACCTG CTCTCGGTGG CCTACAAGAA CGTAGTGGGA

FIG. S5. Nucleotide sequences around the exon-intron boundaries of *ywhag1*. (A) Boundary of exon 1/intron 1. (B) Boundary of intron 1/exon 2. Underlining in (A) indicates the target sequence of the *ywhag1*-spMO.

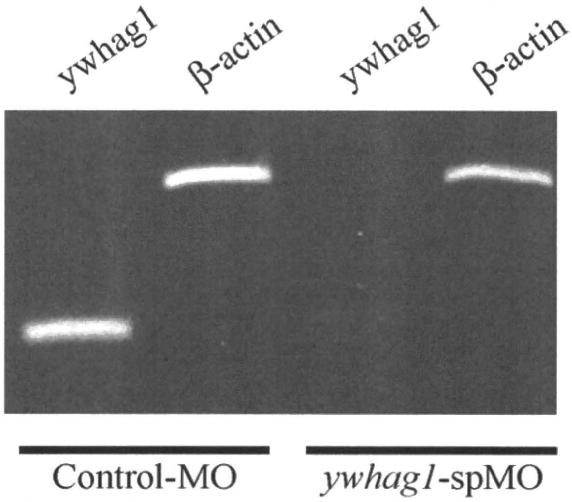

FIG. S6. Estimation of mRNA level in morphants. Microinjection of *ywhag1*-spMO drastically reduced *ywhag1* mRNA.

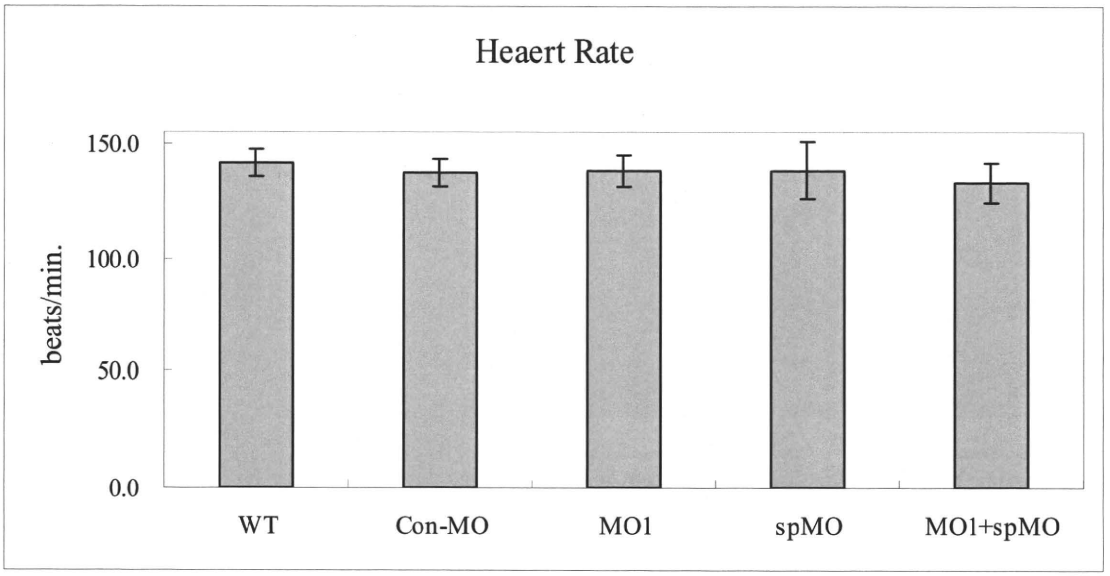

FIG. S7. Comparison of average heart rate of wildtype larvae and control-MO, *ywhag1*-MO1, *ywhag1*-spMO and *ywhag1*-MO1+spMO morphants. Error bar indicates standard deviation of the mean. There are no statistically significant differences among them. N=30 each.

Table S1. Heart Rate of Each Individual Zebrafish.

Individual	WT	Control MO	*ywhag1*-MO1	*ywhag1*-spMO	MO1+spMO
1	148	147	143	154	135*
2	145	144	133	144	146
3	151	134	146*	126	142
4	141	138	120	115	158*
5	140	130	131	94*	118*
6	139	136	133	138	138
7	145	138	116*	116	150*
8	133	152	144	154	96*
9	141	131	151*	144	129
10	135	139	142	142	131
11	142	130	138	141*	141*
12	139	134	148	148*	124
13	141	135	141	138	114
14	144	137	122*	153	121
15	130	142	132*	139*	133*
16	137	132	141	134*	138
17	137	142	143	111	126
18	143	134	128	131	118*
19	138	137	148	125*	134
20	134	133*	125*	132	125
21	153	131	151*	139	128*
22	141	135	98*	151	132*
23	137	131	120*	148	125
24	138	135	137	143	137
25	157	120*	137	135	145
26	139	142	143	120*	114*
27	140	128	104*	137	138
28	145	132	139	137*	129
29	143	136	135	143	143
30	141	146	132	128*	144*
AVE.	141.2	136.7	137.8	137.8	132.5
STDEV	5.8	5.8	6.9	12.5	9.0
No. of arrhythmia	0	2	10	9	12

Asterisk indicates individuals that showed arrhythmia.

Table S2. Primers for PCR and Sequencing of *HIP1* All Exons

	Sense	Antiense
exon 1	CAGAACTCACAGCCAATGGC	CCAGATCTGCACGTCAATGC
exon 2	TGGGCGCCTGCAGAGGAAC	AGAAGCTGCAGGGACCTGGC
exon 3	TGTGATGGCTGGGTGCAGGC	GCAGTGTGGGAGAGGACAGC
exon 4	CATTAGAGTTGGGTGAGTCTCC	TGGAACTTTCCTGAAGCGTCC
exon 5	CCTGGGCAACAGAGCTAGAC	GAAAGAGCTGACAAATGAGCC
exon 6	TGGAGTGCAGTGGCCTTGAAC	AAGCGAGACAGACAGGAAAGC
exon 7	CTGTTGACTTCACCAGGCTGC	CCTTGTGCTGCACACTTTGC
exon 8	GTCCTTGGTGTATGTTGGACC	CCAAAGGCACTGAGAAGGAC
exon 9	GGCAGTGCTGGCCACATGC	TCTTGGCCTCAAGTGATCCTC
exon 10, 11*	TATCTCCTTGACAGCCTGTGC	ACCTGGTTAGAGTCAATGGGC
exon 12	ACAGGTCTGAACCGTTTAATTC	GATGTTCTGTATCTAAGAAGCC
exon 13	CTTGACCCTCAAATATTGGCCC	GCCTGCCAACACACCCGG
exon 14	CTTGGAAGCATGGTAGGACC	CAGCCTCTGTGCCGCATCC
exon 15	TAGGGACCCTGGCTCATTGC	GACGGCAATGCCTTAGAGATC
exon 16	CTCTAGGGCACGCACAGCC	CTGCCCATGGAGCAGAAGGC
exon 17	CTCTTGTTGATCGCTTGGGAC	GGTGGAGGCTGCAGTGAGC
exon 18	GCAGGTTAAAGAGCCATCACC	GAATGTCTGCACAATCAGGCC
exon 19	CCATGACTTGAGCTAAGATGC	TAAGGTAATGCTGACATGCTGC
exon 20	CTTACCCACTAGGTAAGCTCC	TTGATGCAGAGGGACCTGTC
exon 21	AGGCAACTCATACAAGAAAGGC	CAAAGTGCTGGAGTTACAGGC
exon 22	GGGCATGGTGGCGCACC	GCATAAATCACTGCACCCGGC
exon 23	TGGCTTGCAGAAGGTGTTTGC	CCACTGTGCCTGGCAAATTC
exon 24	AGCTACCACACGATGTTGGAC	TGGCTGCTACTGCTCTCCTC
exon 25	CAGCAACCTCAGCACCCTTC	ACAGAGTAAGACGGCAGCATC
exon 26	TAATGCTTATGTCTCAGAGTTAC	GGTCCTATTGACTTCCTGATC
exon 27	TACAAGGGAGCCTGGCTCTC	AGCCAAGTACTGCCTAACGC
exon 28	CCACATATGTTTGCTAAGAACC	TGAAAGAATTTAGACACAGTCC
exon 29	ATTGGCTGCCTCTCAGGTGC	TTAGTAGGTGCACCTGTGTTC
exon 30	TCACTACCAGCCTGGGCAGC	AGAAGGAAGAAGCCACCGATC
exon 31	TAGTCATTCCTAGACACGAAAC	CCTCGGCACTGGGTAATGGC

Since the size of the intron 10 between exon 10 and exon 11 is too small, those are amplified at once.

Table S3. Primers for PCR and Sequencing of *YWHAG* All Exons

	Sense	Antiense
exon 1	CTCAGTGCACTGCAGGTTACAC	CCTTCCACGCCAAGGACCGC
exon 2	AACAGAGCTCTGTTCTAGTGTC	TCTTTGCTGATCTCGTGGGC
exon 3	GACTACTACCGCTACCTGGC	TTCTCCCTGGGAAGGTCATC

Table S4. Primers Used in This study for Zebrafish

Morpholino/Primer Name	Sequence
hip1-MO1	5'-CATTGAACTCTTGACGCGGTCCATT-3'
hip1-MO2	5'-GCGCGAGCGACCAAGACTTCCTAAA-3'
ywhag1-MO1	5'-GTCGACCATGTTCAGTTTTGGG-3'
ywhag1-spMO	5'-TGCAAAAGTTGCGCTTACCGATTTC-3'
Standard Control MO	5'-CCTCTTACCTCAGTTACAATTTATA-3'
*hip1*_F	5'-ATGGACCGCGTCAAGAGTTC-3'
hip1-R	5'-TCTCAACCCGTTCCTTCCTC-3'
*hip1*_5'RACE1	5'-GAGCAGTTTGAGGTAGATGC-3'
*hip1*_5'RACE2	5'-CTTCCAAACTGTTGGCACCG-3'
*hip1*_5'RACE3	5'-GCTGGAAGTTTTGCCACGTC-3'
*hip1*_5'RACE4	5'-CATTAAGGACTCTATGCGGC-3'
*hip1*_5'RACE_RT	5'-GAGCAGTTTGAGGTAGATGC-3'
*hip1*_3'RACE1	5'-GGCTGCAGAAAGAGAGAGACCG-3'
*hip1*_3'RACE2	5'-GACGCTCACCCAGATCAAGAGG-3'
*ywhag1*_5'RACE_RT	5'-GTTGAGCACGTCTTG-3'
*ywhag1*_5'RACE1	5'-CATCATATCTCTCCGCCTGC-3'
*ywhag1*_5'RACE2	5'-GCTTCGTTCAGCTCTGTCAC-3'
*ywhag1*_5'RACE3	5'-CATCGAGCAGAAGACCTCAG-3'
*ywhag1*_5'RACE4	5'-GAAATGGTCCGCGCTTATCG-3'
*ywhag1*_ex1	5'-CCCAAAACTGAACATGGTCG-3'
*ywhag1*_ex2	5'-CTGAGGTCTTCTGCTCGATG-3'
*ywhag1*_int1	5'-CGTTTCAGCAGGACTATACC-3'
*ywhag1*_int2	5'-GACTTCCGGCTACTTTGACG-3'
3'RACE_anchor	5'-GACCACGCGTATCGATGCGAC-3'
oligo d(T)-anchor	5'-GACCACGCGTATCGATGCGACTTTTTTTTTTTTTTTV-3'

V in oligo d(T)- anchor represents A, C or G